Send Orders for Reprints to reprints@benthamscience.net

1022 *Current Topics in Medicinal Chemistry,* **2014**, *14,* **1022-1032**

Modes of Action of Arjunolic Acid and Derivatives on *Trypanosoma cruzi* Cells

Lourdes C. Souza-Neta[1,3,§], Diego Menezes[1,†], Milena S. Lima[3], Martins D. Cerqueira[3], Frederico G. Cruz[3], Dirceu Martins[3] and Marcos A. Vannier-Santos[1,2]*

[1]*Laboratório de Biologia Parasitária, Centro de Pesquisa Gonçalo Moniz, Fundação Oswaldo Cruz - FIOCRUZ, Salvador, BA, Brazil;* [2]*Instituto Nacional para Pesquisa Translacional em Saúde e Ambiente na Região Amazônica, Conselho Nacional de Desenvolvimento Científico e Tecnológico/MCT, Brazil;* [3]*Grupo de Estudo de Produtos Naturais, Instituto de Química, Universidade Federal da Bahia (UFBA), BA, Brazil*

Abstract: Chagas disease causes considerable morbimortality in the Americas, with *circa* 7 to 8 million infected people, causing at least 12,000 annual deaths and 100 million people at risk. Its chemotherapy is poorly selective and effective, associated to severe side effects and unresponsive cases. Thus, R&D on therapeutic alternatives is undoubtedly required. The Brazilian poorly studied biodiversity offers uncountable bioagents, which may be exploited for chemotherapy. The triterpene arjunolic acid (AA), reduced the *Trypanosoma cruzi* epimastigote *in vitro* proliferation with an apparent IC_{50} of 171 μM. Electron microscopy analysis revealed remarkable effects on the parasite surface and architecture. AA-treated parasites displayed minutely corrugated plasma membranes devoid of subpellicular microtubules as well as biogenesis of multiple basal bodies. As the AA effects appeared mainly restricted or originated at the parasite peripheral cytoplasm, including the cytoskeleton membrane linkage, we inferred that the compound targeted primarily the lipid bilayer; therefore, we performed synthetic modification to increase the molecule lipophilicity and thus membrane permeability. The methyl ester (MeAA) and tri-acetylated derivatives (3AcAA) had potentiated trypanocidal activity, producing IC_{50} values of 21.9 and 15.8 μM, respectively. Both derivatives were able to produce remarkable ultrastructural alterations in the parasites, including inner compartments such as Golgi apparatus and the endocytic/autophagic pathway. Parasites cultured with both derivatives displayed numerous and large autophagic vacuoles, altered flagellar length and cell body connection. These data indicate that synthetically-modified natural products comprise valuable tools in antiparasitic chemotherapy and that electron microscopy may be useful not only in determining the mechanisms of action but also in directing such modifications for rational drug design.

Keywords: Chemotherapy, electron microscopy, natural products, triterpene, *Trypanosoma cruzi*.

INTRODUCTION

Chagas disease or American trypanosomiasis affects *circa* 7 to 8 million people in Latin America, and at least 40 million are under risk of infection [1]. Presently the parasite is spreading to other countries, via human transports and it was estimated that there are >300,000 chagasic individuals United States, and >80,000 in Europe [2]. *Trypanosoma cruzi*, the etiological agent of the disease, is exploring new niches emerging in the Brazilian Amazon and exploiting the oral route of transmission [3, 4]. Patients may present cardiopathy with high morbidity and mortality. Treatment of Chagas disease is based on the use of the nitroheterocyclic agents nifurtimox (N-(3-methyl-1,1-dioxo-1,4-thiazinan-4-yl)-1-(5-nitro-2-furyl)methanimine) and benznidazole (N-benzyl-2-(2-nitro-1H-imidazol-1-yl)acetamide), associated with considerable side effects and refractory cases caused by drug-resistant strains [5-7]. In addition, sterile cures are usually not achievable. Therefore, new antitrypanosomal agents are required, but despite the high incidence and mortality of the infection there has been little commercial interest in developing new compounds for the treatment of neglected diseases [8]. Therefore, development of new chemotherapeutic agents by governmental institutions is urgently needed. Natural products obtained from vegetable sources may provide new compounds with antiparasitic activity [9-14].

Arjunolic acid (AA) is an oleanane-type triterpene (Fig. **1**) which was firstly isolated from *Terminalia arjuna* (Combretaceae) and showed many interesting biological activities [15]. It was reported to be an antioxidant, protecting rat myocardium from isoproterenol-induced necrosis and can protect cells from necrosis caused by sodium fluoride-induced oxidative stress [16]. AA exerts protective effect from oxidative stress produced by arsenic in liver [17], kidneys [18], testis

*Address correspondence to this author at the Laboratório de Biologia Parasitária, Centro de Pesquisa Gonçalo Moniz, Fundação Oswaldo Cruz - FIOCRUZ, Rua Waldemar Falcão 121, Candeal, Salvador, BA, Brazil 40296-710; Tel: +55-71-31762208; Fax: +55-71-31762236;
Emails: vannier@bahia.fiocruz.br or marcos.vannier@pesquisador.cnpq.br

[§]***Present Address:*** *Departamento de Ciências Exatas e da Terra I (DCET-I) da Universidade do Estado da Bahia (UNEB).*

[†]***Present Address:*** *Núcleo de Biotecnologia e Bioprospecção- NBBio, Escola Bahiana de Medicina e Saúde Pública- EBMSP, Salvador, BA, Brazil.*

1873-5294/14 $58.00+.00

[19], myocardium [20, 21], and brain [22]. AA presents antibacterial activity against *Escherichia coli*, *Bacillus subtilis* and *Shigella sonnei* [23] and antifungal activity against *Candida albicans*, *Cryptococcus neoformans*, *Aspergillus fumigatus*, *Microsporum canis* and *Sporothrix schenckii* [24]. It is noteworthy that this compound and its derivatives are able to reverse the activation of the Epstein-Barr virus induced by tumor promoter, protein kinase C activator 12-*O*-tetradecanoyl-phorbol-13-acetate [25]. Furthermore, AA antitumoral activity was also reported [26].

Here we compared *in vitro* trypanocidal activity of natural product AA, purified from *Myrcia rotundifolia* (Myrtaceae) as well as of its *per*-acethylated (3AcAA) and methyl ester (MeAA) arjunolic acid derivatives (Fig. **1**) on *T. cruzi* epimastigotes and as the ultrastructural analysis may be useful in the elucidation of trypanocidal compounsds mode of action [27-30] we used electron microscopy to compare the activity of AA and its derivatives on *T. cruzi* subcellular organization and to approach the cell death mechanisms.

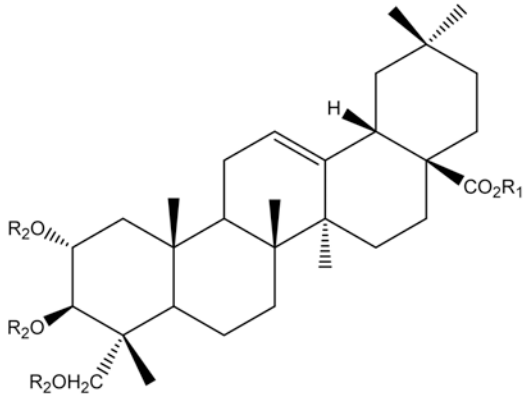

$R_1 = R_2 = H$ arjunolic acid (AA)
$R_1 = Me$; $R_2 = H$ arjunolic acid methyl ester
$R_1 = H$; $R_2 = H_3CCO$ tri-acetylated arjunolic acid (3 AcAA)

Fig. (1). Molecular structure of arjunolic acid (AA) and its methyl ester (MeAA) and tri-acetylated (3AcAA) derivatives.

MATERIALS AND METHODS

Plant Material

M. rotundifolia specimens were collected in the sand dunes of Lagoa do Abaeté Metropolitan Park, Bahia State, Brazil. The plants were identified by Professor Maria Lenise S. Guedes and the voucher specimen (ALCB 52166) is stored at Alexandre Leal Costa Herbarium of the Biology Institute, UFBA.

Extraction and Isolation of the Arjunolic Acid (2α, 3β, 23-Trihydroxyolean-12-en-28-oic Acid)

The dried and powdered *M. rotundifolia* stems (2576 g) were successively extracted three times by maceration with hexane, yielding 4.5 g, and three times maceration with methanol, yielding 78 g. The methanol extract was dissolved in a mixture of methanol and water (8:2) and this solution was successively extracted three times with dichloromethane yielding 10.4 g, and three times with ethylacetate (EtOAc) yielding 4.9 g.

The dichloromethane fraction was subjected to silica gel column chromatography eluted with hexane/EtOAc in increasing polarity, yielding 16 fractions. The combined fractions 13-16 (5.7 g), were fractionated successively by column chromatography, using a gradient of hexane/EtOAc to yield arjunolic acid (0.713 g) which was identified by ^{1}H and ^{13}C NMR.

Preparation of the Methyl Ester and *Per*-acetilated Derivatives of the Arjunolic Acid

The methyl ester of arjunolic acid was obtained after esterification with ethereal diazomethane prepared from Diazald (Aldrich Chemical Co.) in the usual procedure [31].

The *per*-acetylated derivative was obtained quantitatively by acetylation of the arjunolic acid carried out with acetic anhydride in triethylamine with addition of 4-dimethylamino pyridine at room temperature for 24 h [32].

Parasites

Trypanosoma cruzi Y strain epimastigotes were cultured at 28 °C in plastic flasks, containing 5 mL of LIT (liver infusion trypticase) medium inoculated with 5 x 10^5 cells/mL, supplemented with 10% (v/v) fetal calf serum. Cells from the mid-log phase were harvested by centrifugation at 1,000 *g* and washed three times in phosphate-buffered saline (PBS) before experiments. Parasite growth was assessed by daily optical density measurement at 610 nm [33].

Statistical Analysis

Presented data are representative of a minimum of two independent experiments, which yielded analogous results. Significant differences (P<0.05) were tested using of variance analysis (ANOVA) and a posteriori Tukey's test for pair-wise comparisons.

Transmission Electron Microscopy (TEM)

Parasites were fixed in 2.5% glutaraldehyde (Sigma, EM grade) and 5 mM $CaCl_2$ in 0.1 M sodium cacodylate buffer pH 7.2, post-fixed in 1% osmium tetroxide and 0.08% potassium ferricyanide, dehydrated in acetone series and embedded in Polybed resin (Polysciences, Inc). Thin sections (about 80 nm-thick) were obtained with an ultramicrotome (Ultracut E, Leica, Wetzlar, Germany) on a diamond knife (Diatome AG, Biel, Switzerland), collected on copper grids (400 mesh) and stained with 2% uranyl acetate for 20 minutes and 1% lead citrate for 5 minutes and observed under a Zeiss 109 transmission electron microscope, as previously described [33].

Scanning Electron Microscopy (SEM)

Samples were fixed and postfixed as described above, dehydrated in ethanol series, dried by the critical point method in a Balzers apparatus, mounted on stubs and covered with a *circa* 20 nm-thick gold layer, as previously described [34]. Specimens were observed in a JEOL 5310 scanning electron microscope.

RESULTS

TEM and SEM of control (untreated or DMSO-treated) *Trypanosoma cruzi* in axenic culture (Fig. **2**) revealed the typical parasite morphology and surface topography in both epimastigotes (a) and trypomastigotes (b). It is noteworthy that epimastigote, the insect dwelling form, during prolonged culturing differentiate in to trypomastigotes, the developmental form infective to the human host. Under TEM, control parasites displayed the normal cell organization of the protozoan, including reservosomes, the single mitochondrion, kinetoplast, associated to one (c) or two (d) flagellum basal bodies, at early phase of cell division. The characteristic subpellicular microtubules underneath the parasite plasma membrane are also shown (d, inset).

The epimastigote axenic proliferation revealed that AA was poorly trypanocidal with an apparent IC_{50} of 171 μM at 120 h and concentrations equal or above 200 μM significantly ($p<0.05$ or $p<0.01$) diminished parasite survival (Fig. **3**).

We employed SEM in order to approach the effects of the triterpene in *T. cruzi* general morphology (Fig. **4**). Parasites cultured in presence of AA displayed bizarrely-shaped cells, particularly at the flagellum-cell body attachment zone (a, thick arrow) and deflagellated parasites were eventually observed (thin arrow). Many cells presented gross waved parallel arrays on the surface (Fig. **4b**, **c**), suggesting subpellicular microtubule cytoskeleton dysfunction.

We used TEM to evaluate the ultrastructural architecture in parasites cultured with the compound. AA-treated parasites presented finely corrugated cell body and flagellar plasma membranes (Fig. **5a**, **b**). Parasite plasma membranes were mostly devoid of subpellicular microtubules underneath cell surfaces and large assemblies of microtubules were detected in the cytoplasm (Fig. **5c**, **d**). The kinetoplast organization was remarkably altered and multiple basal bodies were detected (Fig. **5e**). Eventually the overall parasite organization was outstandingly altered. Cytoplasmic vacuolization and disorganized organelles were observed as well as of large compartments presenting electrondense fibrillar material (Fig. **5f**, white arrow), presumably of mitochondrial origin, displaying cristae-resembling membrane structures (black arrow) as well as large vacuoles, presenting fibrillary or tubular material, possibly resultant from partially degraded/depolymerized microtubules.

The trypanocidal activities of the methylated (MeAA, a) and acethylated (3AcAA, b) derivatives were significant (*$p<0.05$; ** $p<0.01$, ANOVA and Tukey post-test) at concentrations equal or above 10 and 25μM (Fig. **6**), with apparent IC_{50} values of 15.8 and 21.9 μM, respectively.

Scanning electron microscopy of MeAA-incubated parasites revealed remarkably altered morphology with numerous rounded or distorted cells (Fig. **7a**, **b**), often displaying altered cell body-flagellum attachment zones and cells with flagellar partial detachment (Fig. **7b**, **c**) or depletion (Fig. **7d**). Many cells were smooth surfaced, whereas and some parasites displayed longitudinal grooves (Fig. **7a**, **b**).

Parasites grown in the presence of MeAA presented alterations, including the appearance of swollen Golgi cisternae and large vesicles (Fig. **8a**), eventually, associated to endoplasmic reticulum cisternae, formation of large autophagic vacuoles (Fig. **8b**) and emergence of numerous

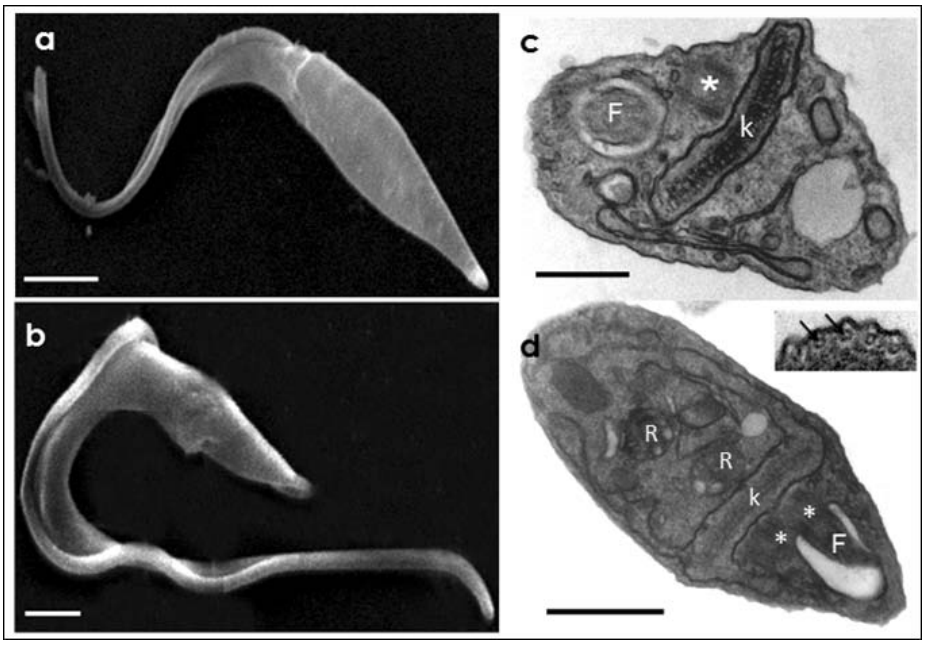

Fig. (2). Scanning (**a, b**) and transmission (**c, d**) electron microscopy of control (untreated or DMSO-treated) *Trypanosoma cruzi* parasites in axenic culture. After prolonged culturing some epimastigotes forms (**a**) differentiate into trypomastigotes (**b**). The normal cell architecture and morphology of the protozoan is displayed. The protozoan single mitochondrion presents typical kinetoplast DNA (**K**) in association with flagellum (**F**) and basal bodies (*****), which may be single (**c**) or duplicated (**d**) at the beginning of cell division. The typical endocytic pathway compartments termed reservosomes (**R**) were observed (**d**). The trypanosomatid plasma membrane is tightly linked to an underneath scaffold of parallel subpellicular microtubules (d- inset, arrows). Bars in (**a**), (**b**) and (**d**) represent 1μm and in (**c**), 0.5 μm.

lipid inclusions (Fig. **8c**). These effects culminated in complete damage of the parasite cell with remarkable loss of cytoplasmic and nuclear material (Fig. **8d**).

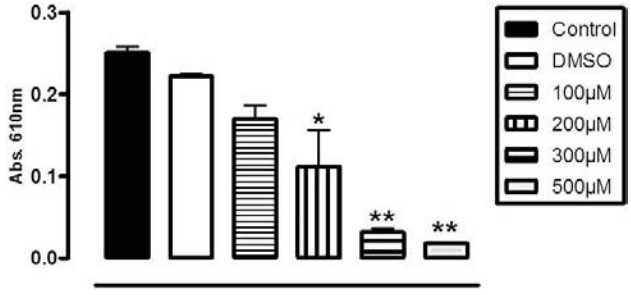

Fig. (3). *T. cruzi in vitro* proliferation before and after different concentrations of arjunolic acid addition. DMSO was used as a solvent control. Cell densities were determined by optical density. At concentrations equal or above 200µM there was significant (* $p<0.05$; ** $p<0.01$, ANOVA and Tukey post-test) inhibition of parasite survival.

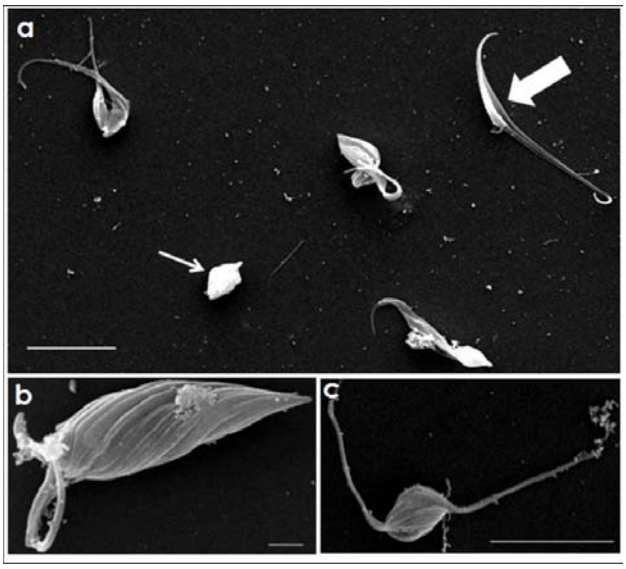

Fig. (4). General morphology of AA-treated *Trypanosoma cruzi* assessed by scanning electron microscopy (SEM). Epimastigotes displayed bizarrely-shaped cells, (**a-c**). Note the distended flagellar attachment zone (**a**, thick arrow) and deflagellated parasites (**a**, thin arrow). Most cells presented wavy parallel longitudinal arrays on the surface (**b, c**), often undergoing irregular cell division processes (**c**), indicating cytoskeletal dysfunction. Bars in (**a**) represent 1µm and in (**b**) and (**c**), 0.5 µm.

The 3AcAA derivative also produced remarkable morphological alterations of parasites assessed by SEM (Fig. **9**). Interestingly the flagellum-cell body attachment zone was remarkably altered and eventually discontinued (Fig. **9a**) and flagella were often stumpy (Fig. **9b**), residual (Fig. **9c**) or even absent (not shown).

Parasites cultured with *per*-acetylated-AA for 96 h presented significant cell architecture alterations assessed by TEM (Fig. **10**). Wide portions of cytoplasm were enveloped by concentric membranes, circumscribing compartments such as mitochondrion-like organelles, lipid inclusions and acidcalcisomes (Fig. **10a**). 3AcAA-treated parasites displayed frequent, large autophagic vacuoles (Fig. **10b**). At advanced stages the compound caused severe parasite cell disorganization, with the formation of massive membrane-bounded, electrolucent areas, secluding the compact residual cytoplasm (Fig. **10c**).

DISCUSSION

Because of pleiotropic beneficial effects on numerous pathological conditions, AA is considered a promising multifunctional therapeutic alternative [15].

Drugs targeting cytoskeleton components may be antitumoral and antiparasitic [35-39]. Microtubule or microfilament-targeting drugs may be used for selecting multidrug resistant phenotypes in both cancer cells and parasites [40-43]. Microtubules comprise useful targets in antikinetoplastid chemotherapy [44, 45].

Triterpenoids may be used for cancer chemoprevention and therapy as well as antiprotozoal agents [46-49]. Although there are several reports on the effects of different natural terpenoids upon different cell types, mostly cancer cells, the cellular effects of arjunolic acid are poorly known.

The observation that arjunolic acid displaces subpellicular microtubules from the *T. cruzi* plasma membrane, remarkably disorganizing the parasite cytoskeleton was surprising since these structures are stabilized by associated proteins and post-translational modifications such as α-tubulin detyrosination which confer the stability to axonemal and subpellicular microtubules. Therefore, the trypanosomatid microtubules are highly resistant to colchicine and benzmidazoles, potent microtubule antagonists in mammalian cells and even destroyed parasites display preserved plasma membrane-microtubule complexes [50-52]. Conversely, parasite protein kinase C (PKC) activation by phorbol ester displaced the *T. cruzi* and *Leishmania* plasma membrane from subpellicular microtubules, forming surface protrusions [53-54]. In this regard AA can modulate PKC [55] and PKC activity can regulate microtubule functioning by phosphorylation of microtubule-associated proteins [56-59], including kinesin and trypanosome kinesins preserve parasite morphology via subpellicular microtubules regulation [60-61].

Furthermore, PKC subcellular localization may be controlled by microtubules [62]. The corrugated appearance of the AA-treated parasite plasma membrane might be due to the action of the triterpenoid on the lateral motility of ergosterol causing the ultrastructural alteration similar the one produced in *Leishmania* surface by the polyene antibiotic filipin, which binds to surface sterols [52, 54]. It is noteworthy that filipin-sterol complexes were shown to be oriented by subpellicular microtubules in *T. cruzi* and *Leishmania mexicana* [63, 64]. Therefore the insertion of AA molecules on the parasite membrane may displace/compete with ergosterol and impair the subpellicular microtubule connection with the plasma membrane. It is remarkable that cholesterol-rich lipid rafts are required for microtubule-mediated surface processes in different cell types [65-67]. Interestingly, besides microtubules and cholesterol, MAP (mitogen-activated protein) kinases (MAPK) may be involved [65], and low

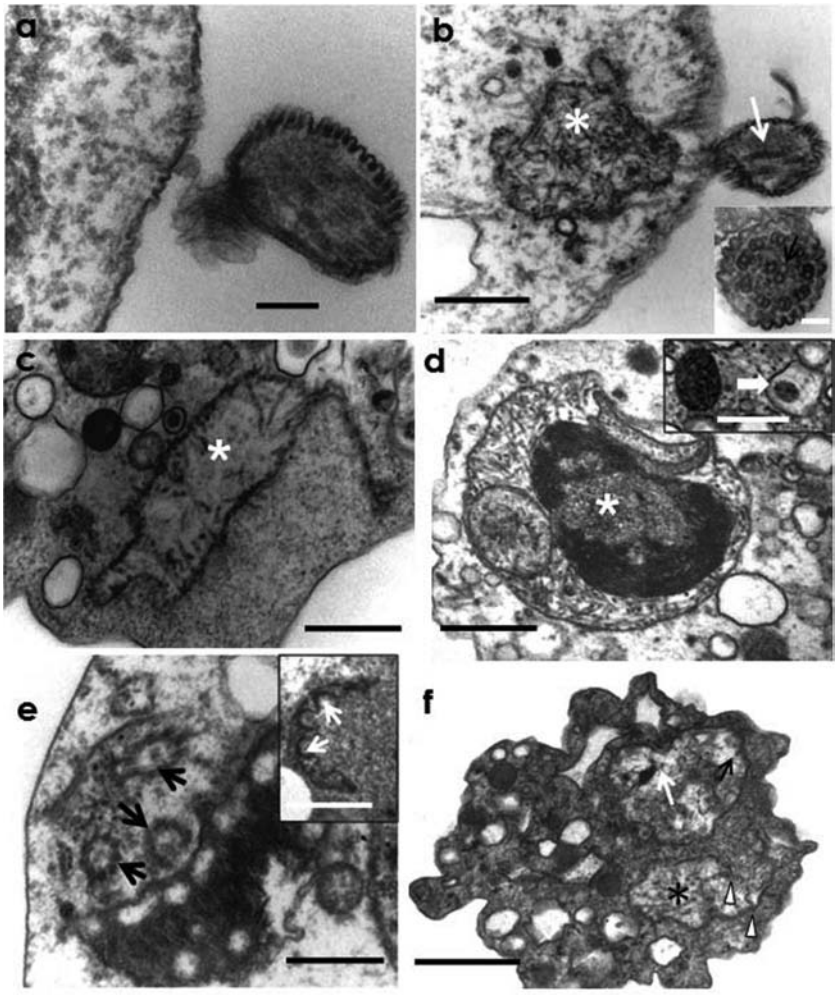

Fig. (5). Transmission electron microscopy (TEM) of AA-treated *T. cruzi* parasites presenting finely corrugated cell body and flagellar plasma membranes (**a**) and the former mostly devoid of subpellicular microtubules (**a, b**). Despite the drastic parasite flagellar surface alterations the axoneme microtubules were often preserved (Figs. **a**), but ectopic microtubules (**b** – inset, black arrow) and eventually overall axoneme disorganization (b, white arrow) were observed. Large cytoplasmic microtubule assemblies were detected in the cytoplasm (Figs. **b-d**, asterisks). Sometimes membrane profiles were associated to microtubule deposits (**c**, arrow) or within membrane-bounded vesicles (d, inset – arrow). Kinetoplast DNA was significantly disordered in AA-treated parasites (**e**). Multiple basal bodies (Fig. **e**, black arrows and inset, white arrows) were often observed and the k-DNA presented atypical compactness. Eventually the overall parasite organization was outstandingly altered (**f**). Cytoplasmic vacuolization and compartments presenting tubular material (*****) were seen, associated with membranes (arrowheads). We notice disorganized compartments of a mitochondria-like appearance presenting electrondense fibrillar material (white arrow) as well as cristae-like digitform membrane profiles (black arrow). Bars in (**a**) and inset in (**b**) represent 0.2 μm and in (**b**) to (**e**), 0.5 μm and in (**f**), 1.0 μm.

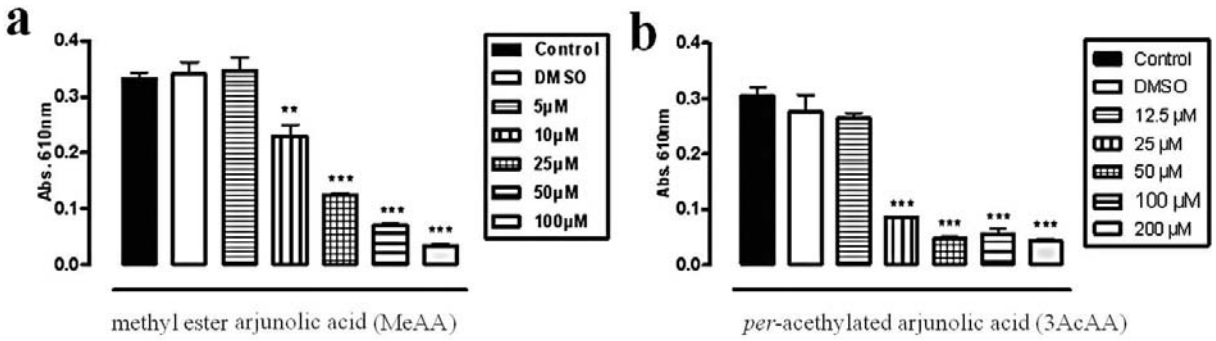

Fig. (6). *T. cruzi in vitro* proliferation before and after addition methylated (**a**) and *per*-acetylated (**b**) arjunolic acid derivatives, using DMSO as a solvent control. Cell densities were determined by optical density. At concentrations equal or above 10 (MeAA) or 25μM (3AcAA) there were significant (** $p<0.05$; *** $p<0.01$, ANOVA and Tukey post-test) inhibition of parasite survival. The apparent IC_{50} were 15.8 and 21.9 μM, respectively.

membrane cholesterol levels activate ERK (extracellular signal-regulated kinases) 1/2 MAPK, leading to the phosphorylation of tau [68]. MAPK (*vide infra*) takes part in the leishmanicidal activity of the triterpenoid 18β-glycyrrhetinic acid [69].

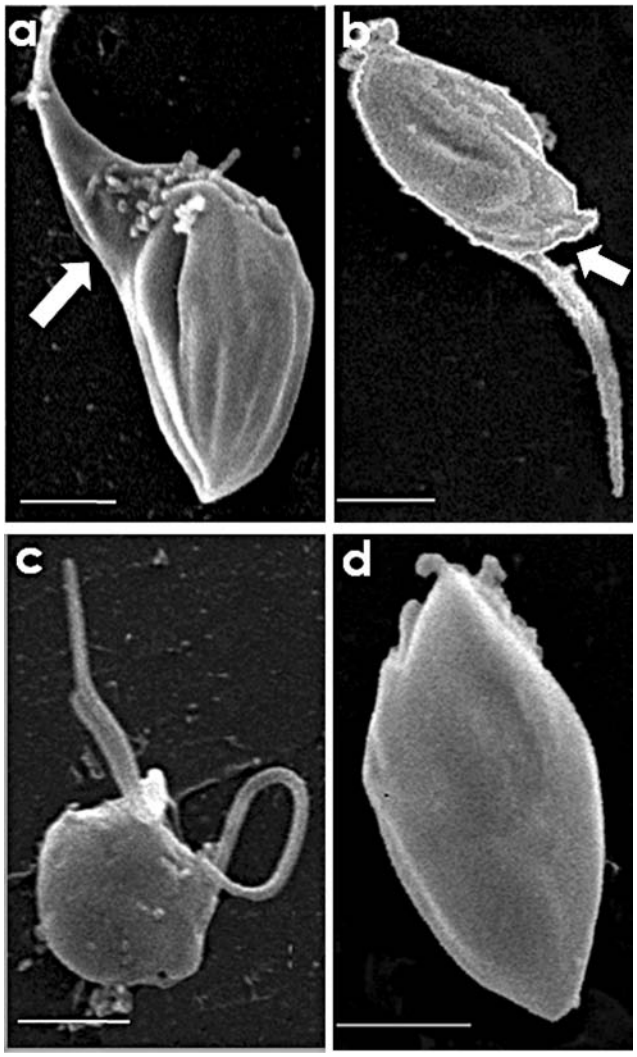

Fig. (7). SEM of *T. cruzi* epimastigotes incubated with methylated AA (MeAA) for 96 hs revealed remarkably altered cell morphology. Several parasite cells displayed enlarged and/or distended flagellar attachment zones (**a**, arrow), partial flagellar detachment (**b**, arrow), which may cause long areas of free flagellum (**c**), culminating in complete deflagellation (**d**). Bars in (**a**) and (**c**) represent 0.5 μm and in (**b**) and (**d**), 1.0 μm and 0.2 μm, respectively.

Phosphorylation of microtubule-associated proteins might lead to their detachment from membranes and triterpenoids such as bufalin were shown to disorganize microtubule usual arrays in mammalian cells, forming perinuclear aggregates [70-72].

Steroidal molecules were reported to disorganize microtubules and microfilaments and the triterpenoid tubeimoside I recognizes the colchicine binding site of tubulin [73-77]. Therefore, the action of the AA could result from the impaired recognition of tubulin by microtubule-binding protein at centrosomes as well as on the plasma membrane.

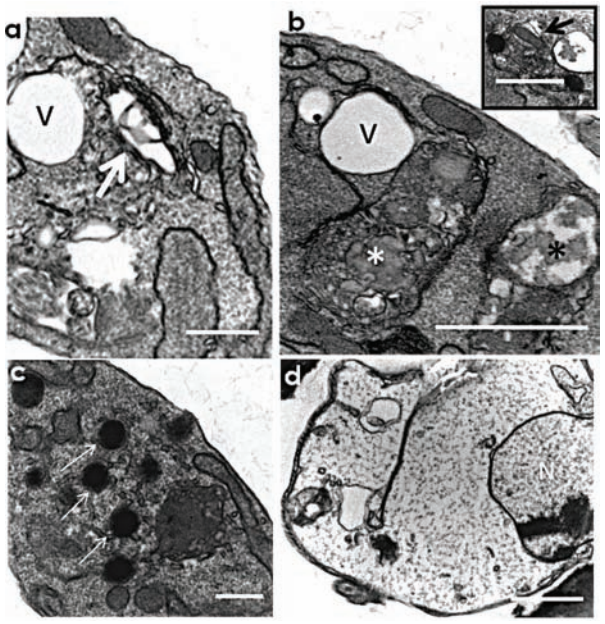

Fig. (8). *T. cruzi* epimastigotes cultured with the methylated-AA derivative for 96h. Many MetAA-treated parasites displayed swollen Golgi apparatus cisternae (**a**, white arrow) and formation of large vacuoles (V). Large autophagic vacuoles (**b**, white asterisk) were frequently formed and partially degraded material could be detected within some of them (**b**, black asterisk), inset shows a mitochondria-like organelle within a vesicle (arrow), indicating macroautophagy. Some parasites presented numerous lipid inclusions (**c** – arrows). These alterations culminated in the total destruction of the parasite cell with remarkable loss of cytoplasmic and nuclear (N) material (**d**). Bars in (**a**) and (**c**) represent 0.5 μm and the remaining bars, 1.0 μm.

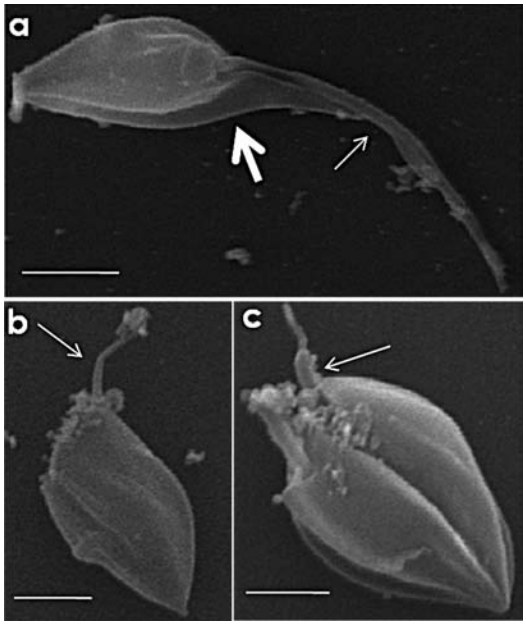

Fig. (9). SEM of *T. cruzi* epimastigotes cultured with acetylated-AA for 96h. We observed remarkably distented (**a**, thick arrow) and eventually discontinuous (**a**, thin arrow) flagellum-cell body attachment zones. Many parasite cells presented only small (**b**, arrow) or residual (**c**, arrow) flagella. Bars in (**a**) represent 1.0 μm and in (**b**) and (**c**), 0.5 μm.

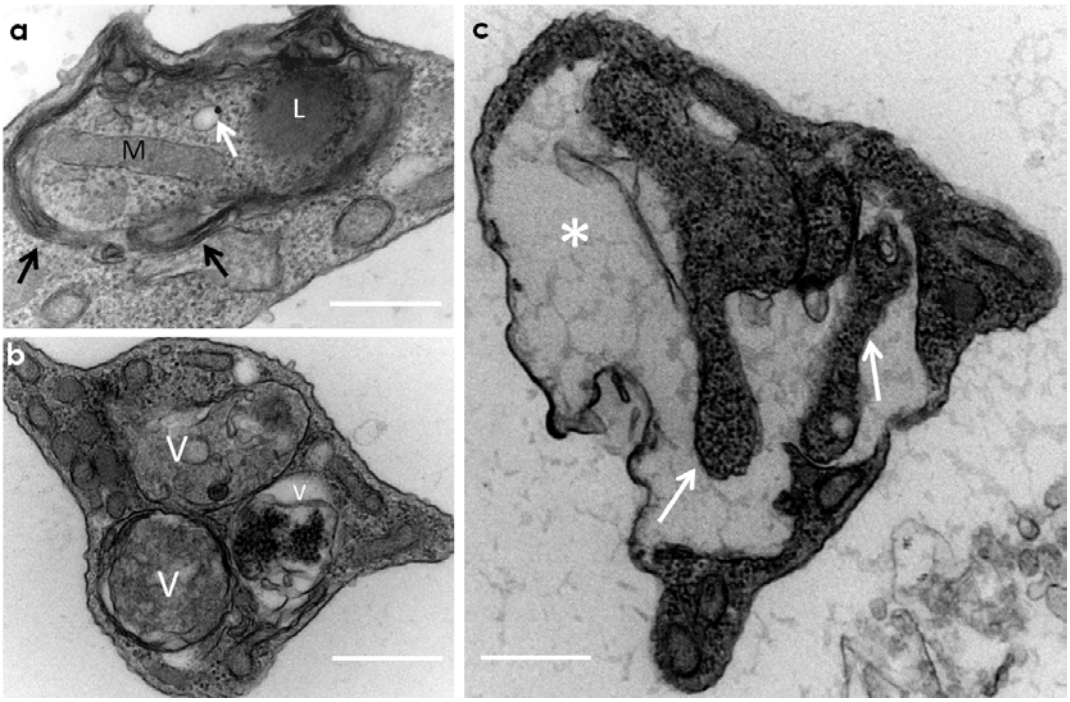

Fig. (10). TEM of *T. cruzi* epimastigotes cultured with acetylated-AA for 96 hs displayed remarkable ultrastructural alterations. Multiple myelin-like membranes (**a** - black arrows) were observed enveloping portions of cytoplasm including a mitochondrion segment (**M**), lipid inclusion (**L**) and acidcalcisome-like compartment (white arrow). Numerous, large autophagic vacuoles (**V**) were observed (**b**). These effects led to drastic changes in cell structure, including massive cytoplasmic loss (**C, ***) and formation of, membrane-bounded, secluded remnant cytoplasm (arrows). Bars in (**a**) and (**b**) represent 0.5 μm and in and (**c**), 1.0 μm.

The cytoskeleton-targeting properties are involved in their cytotoxocity upon different cell types. The detailed mechanism of action of this compound has not been determined but it is noteworthy that estrogen is able to destabilize microtubules via ion channel transient receptor potential, vanilloid subclass I [78].

The microtubute bundling effect apparently depends on ERK 1/2 activity and Na^+-K^+ATPase phosphorylation [79], which crosstalk [80]. In this regard, plasma membrane cholesterol levels reciprocally regulate α1 Na/K-ATPase and the extracellular K^+ levels can modulate ERK 1/2 activation [81]. In addition the leishmanial PKC-like protein kinase modulates was demonstrated to regulate Na^+-K^+ATPase [82].

MAPK such as ERK were formerly known to regulate cell division, but several other cellular functions may be attributed to this versatile enzyme family [83]. Mammalian ERK takes part in leishmanial infection affecting responses by different cell types [84-86]. Parasite MAPK account for considerable part of the Trypanosomatid kinome and thus comprise chemotherapy targets and vaccine candidates [87-90].

MAPK activity may underlie several cellular phenomena including Flagellum-associated MAPK co-participate it the flagellar length regulation which is controlled by a process called intraflagellar transport (IFT) by dynein and kinesin protein motors [91]. The reduced flagellar length in AA-treated *T. cruzi* may be related to the parasite MAPK activity or motor protein function.

The flagellum attachment zone (FAZ) plays important but previously overlooked roles. The FAZ positioning controls cleavage furrow formation in *T. brucei* [92]. The *T. cruzi* FAZ is associated to linearly arrayed integral membrane proteins, connecting the flagellar and cell body membranes [93].

In the trypanosomatid protozoan *Leishmania amazonensis*, both FAZ and ciliary necklace, which is found in the vicinity of basal bodies in the transition zone, displayed intense tyrosine phosphorylation [94], indicating that local signaling events take place in this complex parasite surface-cytoskeleton linkage domain.

Cilia and flagella were previously viewed simply as undolipodia responsible for cell motility. Recent evidence indicate that cilia and centrosomes are involved on cell cycle signaling regulation displaying enzymes involved in the mitotic regulation [95, 96]. Flagellum-kinetoplast connection plays a pivotal role in *Trypanosoma* morphogenesis, cell division and differentiation [97].

Cytoskeleton disorganizations triggered by altered microtubule binding capacity could presumably deregulate mitochondrial genome division. Alternatively, the triterpenoid derivative could target DNA topoisomerases as dihydrobetulinic acid does in *Leishmania donovani* [48].

The cytoskeleton functioning was shown to be required for mitochondrial genome segregation [98, 99], therefore the disorganized k-DNA in parasites cultivated with MeAA may

indicate the microtubule disorganization causes impaired cell division.

Interestingly the primary cilium found in most mammalian cell types emerges from a ciliary pocket with morphologic and functional similarities with the trypanosomatid flagellar pocket [100-103]. In both mammalian and kinetoplastid cells these surface structures accomplish sensory roles [91, 104] and may be related to autophagy [105].

The calcium-activated microtubule-severing ATPase katanin [106, 107], and FA1 and FA2 serine/threonine NIMA (Never In Mitosis) kinases are involved in *Chlamydomonas reinhardtii* deflagellation [108].

Stress and extracellular stimuli may disrupt calcium homeostasis causing deflagellation in eukaryotic cells [109]. The calcium entry from the extracellular milieu was not approached here and cannot be excluded presently but, microtubule severing could not completely explain the *T. cruzi* deflagellation triggered by methylated AA derivative observed by SEM indicate that the disrupture of the FAZ comprises an early event preceding the flagellar loss observed here. Similar images of flagellar detachment were observed in *T. brucei* after RNAi-mediated centrin 1 depletion [110], raising the possibility of centrosome involvement in flagellar detachment. As basal bodies promote the cilia/flagella ontogenesis, the organelle disorganization may lead to the appearance of small flagella and/or deflagellation in AA-treated *T. cruzi*, revealed by SEM.

The centrosome disorganization may be caused by cytoskeleton dysfunction as microtubule depolymerization by nocodazole was shown to cause centrosome splitting in human tumor cells [111]. The centrosome targeting of the bioagent studied here may be relevant for antitumoral interventions as centrosomes may comprise targets for cancer chemotherapy [112]. Centrosome cohesion is regulated by a balance of kinase and phosphatase activities. The centrosome amplification may be caused by centriole disengagement which may be brought by disfunction of molecules such as cohesin (reviewed in [113]). In kinetoplastid protozoa the kDNA is physically connected to and is segregated by the flagellar basal bodies therefore, the basal body disorganization could impair mitochondrial duplication and consequently, trypanosomatid parasite proliferation [95, 114].

AA has low antiparasitic activity against *L. amazonensis* [49], but changes such as *per*-acetylation and methylation were able to significantly increase the AA trypanocidal effect, presumably by enhancing the molecule hydrophobicity and therefore plasma membrane permeability. The activity of theses derivatives apparently is largely dependent on autophagy as numerous and massive autophagic vacuoles were observed on both MeAA and 3AcAA. The presence of numerous lipid inclusions in the cytoplasm of MeAA may be an outcome of the autophagic process as reported in parasites cultured with ergosterol biosynthesis inhibitors [115, 116]. The terpenoids were shown to induce autophagy in mammalian cells [117-120], which may be associated with generation of reactive oxygen species [121], nevertheless, AA was shown to be an antioxidant [15]. Curiously, contrary to cholesterol, sitosterol can promote autophagy [122].

Autophagy induction may diminish the macrophage phagocytic activity and it may modulate leishmanial infection [123], but this phenomenon was not studied on trypanosomatid parasites.

Taken together these results indicate that microtubule-targeting compounds may comprise trypanocidal agents and group substitution in natural products, evaluated via electron microscopy for structure-activity relation [124, 125], may lead to identification of target subcellular compartments and/or metabolic pathways as well as pharmacophoric groups to be exploited in antiparasitic chemotherapy.

CONFLICT OF INTEREST

There is no interest conflicts concerning the present research and all authors agree with its publication in the present form.

ACKNOWLEDGEMENTS

This work was supported by CNPq/MCT, FINEP, PROCAD-NF Capes, PP-SUS, FAPESB, INCT-INPeTAm. MAVS is a CNPq research fellow.

LIST OF ABBREVIATIONS

3AcAA	=	Tri-acetylated arjunolic acid
AA	=	Arjunolic acid
ANOVA	=	Variance analysis
DMSO	=	Dimethyl sulfoxide
ERK	=	Extracellular signal-regulated kinases
EtOAc	=	Ethylacetate
FAZ	=	Flagellum attachment zone
IFT	=	Intraflagellar transport
LIT	=	Liver infusion trypticase
MAP	=	Mitogen-activated protein
MAPK	=	Mitogen-activated protein kinase
MeAA	=	Arjunolic acid methyl ester
NIMA	=	Never in mitosis
NMR	=	Nuclear magnetic resonance
PBS	=	Phosphate-buffered saline
PKC	=	Protein Kinase C
R&D	=	Research and development
SEM	=	Scanning electron microscopy
TEM	=	Transmission electron microscopy

REFERENCES

[1] World Health Organization (WHO) Chagas disease (American trypanosomiasis) Fact sheet N°340, **2014**.

[2] Coura, J.R.; Viñas, P.A. Chagas disease: a new worldwide challenge. *Nature*, **2010**, *465*, S6-7.

[3] Coura, J.R.; Junqueira, A.C.V.; Fernandes, O.; Valente, S.A.S.; Miles, M.A. Emerging Chagas disease in Amazonian Brazil. *Trends Parasitol.*, **2002**, *18*, 171-176.

[4] Dias, J.P.; Bastos, C.; Araújo, E.; Mascarenhas, A.V.; Martins Netto, E.; Grassi, F.; Silva, M.; Tatto, E.; Mendonça, J.; Araújo, R.F.; Shikanai-Yasuda, M.A.; Aras, R.A. Chagas disease outbreak associated with oral transmission. *Rev. Soc. Bras. Med. Trop*., **2008**, *41*, 296-300.

[5] Castro, J.A.; de Mecca, M.M.; Bartel, L.C. Toxic side effects of drugs used to treat Chagas' disease (American trypanosomiasis). *Hum. Exp. Toxicol.*, **2006**, *25*, 471-479.

[6] Filardi, L.S.; Brener, Z. Susceptibility and natural resistance of *Trypanosoma cruzi* strains to drugs used clinically in Chagas disease. *Trans. Roy. Soc. Trop. Med. Hyg*., **1987**, *81*, 755-759.

[7] Camandaroba, E.L.; Reis, E.A.; Gonçalves, M.S.; Reis, M.G.; Andrade, S.G. *Trypanosoma cruzi*: susceptibility to chemotherapy with benznidazole of clones isolated from the highly resistant Colombian strain. *Rev. Soc. Bras. Med. Trop*., **2003**, *36*, 201-209.

[8] Trouiller, P.; Olliaro, P.; Torreele, E.; Orbinski, J.; Laing, R.; Ford, N. Drug development for neglected diseases: a deficient market and a public-health policy failure. *Lancet*, **2002**, *359*, 2188-2194.

[9] Kayser, O.; Kiderlen, A.F.; Croft, S.L. Natural products as antiparasitic drugs. *Parasitol. Res.*, **2003**, *90*, 55-62.

[10] Balunas, M.J.; Kinghorn, A.D. Drug discovery from medicinal plants. *Life Sci*., **2005**, *78*, 431-441.

[11] Tempone AG[1], Borborema SE, de Andrade HF Jr, de Amorim Gualda NC, Yogi A, Carvalho CS, Bachiega D,Lupo FN, Bonotto SV, Fischer DC. Antiprotozoal activity of Brazilian plant extracts from isoquinoline alkaloid-producing families. *Phytomedicine*, **2005**, *12*(5), 382-390.

[12] Salem, M.M.; Werbovetz, K.A. Natural products from plants as drug candidates and lead compounds against leishmaniasis and trypanosomiasis. *Curr. Med. Chem*., **2006**, *13*, 2571-2598.

[13] Itokawa, H.; Morris-Natschke, S.L.; Akiyama, T.; Lee, K.H. Plant-derived natural product research aimed at new drug discovery. *Nat. Med*., **2008**, *62*, 263-280.

[14] Potterat, O.; Hamburger, M. Drug discovery and development with plant-derived compounds. *Prog. Drug Res*., **2008**, *65*, 47-118.

[15] Ghosh, J.; Sil, P.C. Arjunolic acid: A new multifunctional therapeutic promise of alternative medicine. *Biochimie*, **2013,** *95*, 1098-1109.

[16] Ghosh, J.; Das, J.; Manna, P.; Sil, P.C. Cytoprotective effect of arjunolic acid in response to sodium fluoride mediated oxidative stress and cell death via necrotic pathway. *Toxicol. in Vitro*, **2008**, *22*, 1918-1926.

[17] Manna, P.; Sinha, M.; Sil, P.C. Protection of arsenic-induced hepatic disorder by arjunolic acid. *Basic Clin. Pharmacol. Toxicol.*, **2007**, *101*, 333-338.

[18] Sinha, M.; Manna, P.; Sil, P.C. Arjunolic acid attenuates arsenic-induced nephrotoxicity. *Pathophysiology*, **2008**, *15*, 147-156.

[19] Manna, P.; Sinha, M.; Sil, P.C. Protection of arsenic-induced testicular oxidative stress by arjunolic acid. *Redox Rep*., **2008**, *13*, 67-77.

[20] Sumitra, M.; Manikandan, P.; Kumar, D.A; Arutselvan, N.; Balakrishna, K.; Manohar, B.M.; Puvanakrishnan, R. Experimental myocardial necrosis in rats: role of arjunolic acid on platelet aggregation, coagulation and antioxidant status. *Mol. Cell Biochem.*, **2001**, *224*, 135-142.

[21] Manna, P.; Sinha, M.; Sil, P.C. Arsenic-induced oxidative myocardial injury: protective role of arjunolic acid. *Arch. Toxicol.*, **2008**, *82*, 137-149.

[22] Sinha, M.; Manna, P.; Sil, P.C. Protective effect of arjunolic acid against arsenic-induced oxidative stress in mouse brain. *J. Biochem. Mol. Toxicol.*, **2008**, *22*, 15-26.

[23] Djoukeng, J.D.; Abou-Mansour, E.; Tabacchi, R.; Tapondjou, A.L.; Bouda, H.; Lontsi, D. Antibacterial triterpenes from *Syzygium guineense* (Myrtaceae). *J. Ethnopharmacol.*, **2005**, *101*, 283-286.

[24] Masoko, P.; Mdee, L.K.; Mampuru, L.J.; Eloff, J.N. Biological activity of two related triterpenes isolated from *Combretum nelsonii* (Combretaceae) leaves. *Nat. Prod. Res.*, **2008**, *22*, 1074-1084.

[25] Diallo, B.; Vanhaelen, M.; Vanhaelen-Fastré, R.; Konoshima, T.; Kozuka, M.; Tokuda, H. Studies on inhibitors of skin-tumor promotion. inhibitory effects of triterpenes from *Cochlospermum tinctorium* on Epstein-Barr virus activation. *J. Nat. Prod*., **1989**, *52*(4), 879–881.

[26] Ajees, A.A.; Balakrishna, K. Arjunolic acid. *Acta Cryst.*, **2002**, *58*, 0682-0684.

[27] De Souza, W. From the cell biology to the development of new chemotherapeutic approaches against trypanosomatids: dreams and reality. *Kinetoplastid Biol. Dis*., **2002**, *31*, 1:3.

[28] Menna-Barreto, R.F; Salomão, K.; Dantas, A.P.; Santa-Rita, R.M.; Soares, M.J.; Barbosa, H.S.; de Castro, S.L. Different cell death pathways induced by drugs in *Trypanosoma cruzi*: an ultrastructural study. *Micron*, **2009**, *40*, 157-68.

[29] Vannier-Santos, M.A.; De Castro, S.L. Electron microscopy in antiparasitic chemotherapy: a (close) view to a kill. *Curr. Drug Targets*, **2009**, *10*, 246-260.

[30] Adade, C.M.; Souto-Padrón, T. Contributions of ultrastructural studies to the cell biology of trypanosmatids: targets for antiparasitic drugs. *Open Parasitol. J.*, **2010**, *4*, 178-187.

[31] Black, T.H. The preparation and reactions of diazomethane. *Aldrichimica Acta*, **1983**, *16*, 3-10.

[32] Mc Murry, J.E; Musser, J.H.; Ahmad, M.S.; Blaszczak, L.C. Total synthesis of eremophilone. *J. Org. Chem.*, **1975**, *40*, 1829-1832.

[33] Menezes, D.; Valentim, C.; Oliveira, M.F.; Vannier-Santos, M.A. Putrescine analogue cytotoxicity against *Trypanosoma cruzi*. *Parasitol. Res*., **2006**, *98*, 99-105.

[34] Maia, C.; Lanfredi-Rangel, A.; Santana-Anjos, K.G.; Oliveira, M.F.; De Souza, W.; Vannier-Santos, M.A. Effects of a putrescine analog on *Giardia lamblia*. *Parasitol. Res.*, **2008**, *103*, 363-370.

[35] Zhou, J.; Giannakakou, P. Targeting microtubules for cancer chemotherapy. *Curr. Med. Chem. Anticancer Agents*, **2005**, *5*, 65-71.

[36] Feng, R.; Li, S.; Lu, C.; Andreas, C.; Stolz, D.B.; Mapara, M.Y.; Lentzsch, S. Targeting the microtubular network as a new antimyeloma strategy. *Mol. Cancer Ther*., **2011**, *10*, 1886-1896.

[37] Bell, A.; Wernli, B.; Franklin, R.M. Effects of microtubule inhibitors on protein synthesis in *Plasmodium falciparum*. *Parasitol. Res.*, **1993**, *79*, 146-152.

[38] Fong, D. Effect of the anti-microtubule compound tubulozole on *Leishmania* protozoan parasites *in vitro*. *FEMS Microbiol. Lett.*, **1993**, *107*, 95-99.

[39] Kappes, B.; Rohrbach, P. Microtubule inhibitors as a potential treatment for malaria. *Future Microbiol.*, **2007**, *2*, 409-423.

[40] Gouazé, V.; Yu, J.Y.; Bleicher, R.J.; Han, T.Y.; Liu, Y.Y.; Wang, H.; Gottesman, M.M.; Bitterman, A.; Giuliano, A.E.; Cabot, M.C. Overexpression of glucosylceramide synthase and P-glycoprotein in cancer cells selected for resistance to natural product chemotherapy. *Mol. Cancer Ther*., **2004**, *3*, 633-639.

[41] Gueiros-Filho, F.J.; Viola, J.P.; Gomes, F.C.; Farina, M.; Lins, U.; Bertho, A.L.; Wirth, D.F.; Lopes, U.G. *Leishmania amazonensis*: multidrug resistance in vinblastine-resistant promastigotes is associated with rhodamine 123 efflux, DNA amplification, and RNA overexpression of a *Leishmania* mdr1 gene. *Exp. Parasitol.*, **1995**, *81*, 480-490.

[42] Borges, V.M.; Lopes, U.G.; De Souza, W.; Vannier-Santos, M.A. Cell structure and cytokinesis alterations in multidrug-resistant *Leishmania* (*Leishmania*) *amazonensis*. *Parasitol. Res.*, **2005**, *95*, 90-96.

[43] Morgan, R.E.; Ahn, S.; Nzimiro, S.; Fotie, J.; Phelps, M.A.; Cotrill, J.; Yakovich, A.J.; Sackett, D.L.; Dalton, J.T.; Werbovetz, K.A. Inhibitors of tubulin assembly identified through screening a compound library. *Chem. Biol. Drug Des.*, **2008**, *72*, 513-524.

[44] Jayanarayan, K.G.; Dey, C.S. Microtubules: dynamics, drug interaction and drug resistance in *Leishmania*. *J. Clin. Pharm. Ther*., **2002**, *27*, 313-320.

[45] Morgan, R.E.; Werbovetz, K.A. Selective lead compounds against kinetoplastid tubulin. *Adv. Exp. Med. Biol.*, **2008**, *625*, 33-47.

[46] Bishayee, A.; Ahmed, S.; Brankov, N.; Perloff, M. Triterpenoids as potential agents for the chemoprevention and therapy of breast cancer. *Front. Biosci.*, **2011**, *16*, 980-996.

[47] Patlolla, J.M.; Rao, C.V. Triterpenoids for cancer prevention and treatment: current status and future prospects. *Curr. Pharm. Biotechnol.*, **2012**, *13*, 147-155.

[48] Chowdhury, A.R.; Mandal, S.; Goswami, A.; Ghosh, M.; Mandal, L.; Chakraborty, D.; Ganguly, A.; Tripathi, G.; Mukhopadhyay, S.; Bandyopadhyay, S.; Majumder, H.K. Dihydrobetulinic acid induces apoptosis in *Leishmania donovani* by targeting DNA topoisomerase I and II: implications in antileishmanial therapy. *Mol. Med.*, **2003**, *9*, 26-36.

[49] Torres-Santos, E.C.; Lopes, D.; Oliveira, R.R.; Carauta, J.P.; Falcao, C.A.; Kaplan, M.A.; Rossi-Bergmann, B. Antileishmanial activity of isolated triterpenoids from *Pourouma guianensis*. *Phytomedicine*, **2004**, *11*, 114-120.

[50] Vedrenne, C.; Giroud, C.; Robinson, D.R.; Besteiro, S.; Bosc, C.; Bringaud, F.; Baltz, T. Two related subpellicular cytoskeleton-associated proteins in *Trypanosoma brucei* stabilize microtubules. *Mol. Biol. Cell*, **2002**, *13*, 1058-1070.

[51] Gull, K. The cytoskeleton of trypanosomatid parasites. *Annu. Rev. Microbiol.*, **1999**, *53*, 629-655.

[52] Pimenta, P.F.; dos Santos, M.A.; de Souza, W. Fine structure and cytochemistry of the interaction between *Leishmania mexicana amazonensis* and rat neutrophils and eosinophils. *J. Submicrosc. Cytol.*, **1987**, *19*, 387-395.

[53] de Carvalho, T.U.; de Souza, W. Effect of phorbol-12-myristate-13-acetate (PMA) on the fine structure of *Trypanosoma cruzi* and its interaction with activated and resident macrophages. *Parasitol. Res.*, **1987**, *74*, 11-17.

[54] Vannier-Santos, M.A.; Pimenta, P.F.; De Souza, W. Effects of Phorbol ester on *Leishmania mexicana amazonensis*: an ultrastructural and cytochemical study. *J. Submicrosc. Cytol. Pathol.*, **1988**, *20*, 583-593.

[55] Ainsztein, A.M.; Purich, D.L. Stimulation of tubulin polymerization by MAP-2. Control by protein kinase C-mediated phosphorylation at specific sites in the microtubule-binding region. *J. Biol. Chem.*, **1994**, *269*, 28465-28471.

[56] Manna, P.; Sinha, M.; Sil, PC. Prophylactic role of arjunolic acid in response to streptozotocin mediated diabetic renal injury: activation of polyol pathway and oxidative stress responsive signaling cascades. *Chem. Biol. Interact.*, **2009**, *181*, 297-308.

[57] Silverman-Gavrila, R.; Silverman-Gavrila, L.; Hou, G.; Zhang, M.; Charlton, M.; Bendeck, M.P. Rear polarization of the microtubule-organizing center in neointimal smooth muscle cells depends on PKCα, ARPC5, and RHAMM. *Am. J. Pathol.*, **2011**, *178*, 895-910.

[58] Schober, J.M.; Kwon, G.; Jayne, D.; Cain, J.M. The microtubule-associated protein EB1 maintains cell polarity through activation of protein kinase C. *Biochem. Biophys. Res. Commun.*, **2012**, *417*, 67-72.

[59] Zhao, H.; Yao, X.; Wang, T.X.; Jin, W.M.; Ji, Q.Q.; Yang, X.; Duan, Q.H.; Yao, L.J. PKCα regulates vasopressin-induced aquaporin-2 trafficking in mouse kidney collecting duct cells in vitro via altering microtubule assembly. *Acta Pharmacol. Sin.*, **2012**, *33*, 230-236.

[60] Sarkar, S.; Bananis, E.; Nath, S.; Anwer, M.S.; Wolkoff, A.W.; Murray, J.W. PKCzeta is required for microtubule-based motility of vesicles containing the ntcp transporter. *Traffic*, **2006**, *7*, 1078-1091.

[61] Hu, H.; Hu, L.; Yu, Z.; Chasse, A.E.; Chu, F.; Li, Z. An orphan kinesin in trypanosomes cooperates with a kinetoplastid-specific kinesin to maintain cell morphology through regulating subpellicular microtubules. *J. Cell Sci.*, **2012**, *1*(125), 4126-4136.

[62] Dykes, A.C.; Fultz, M.E.; Norton, M.L.; Wright, G.L. Microtubule-dependent PKC-alpha localization in A7r5 smooth muscle cells. *Am. J. Physiol. Cell Physiol.*, **2003**, *285*, C76-87.

[63] Souto-Padrón, T.; de Souza, W. Freeze-fracture localization of filipin-cholesterol complexes in the plasma membrane of *Trypanosoma cruzi*. *J. Parasitol.*, **1983**, *69*, 129-137.

[64] Pimenta, P.F.; de Souza, W. *Leishmania mexicana*: distribution of intramembranous particles and filipin sterol complexes in amastigotes and promastigotes. *Exp. Parasitol.*, **1987**, *63*, 117-135.

[65] Huang, W.R; Wang, Y.C.; Chi, P.I.; Wang, L.; Wang, C.Y.; Lin, C.H.; Liu, H.J. Cell entry of avian reovirus follows a caveolin-1-mediated and dynamin-2-dependent endocytic pathway that requires activation of p38 mitogen-activated protein kinase (MAPK) and Src signaling pathways as well as microtubules and small GTPase Rab5 protein. *J. Biol. Chem.*, **2011**, *286*, 30780-30794.

[66] Xu, X.; Warrington, A.E.; Wright, B.R.; Bieber, A.J.; Van Keulen, V.; Pease, L.R.; Rodriguez, M. A human IgM signals axon outgrowth: coupling lipid raft to microtubules. *J. Neurochem.*, **2011**, *119*, 100-112.

[67] Schober, J.M.; Kwon, G.; Jayne, D.; Cain, J.M. The microtubule-associated protein EB1 maintains cell polarity through activation of protein kinase C. *Biochem. Biophys. Res. Commun.*, **2012**, *417*, 67-72.

[68] Sawamura, N.; Gong, J.S.; Chang, T.Y.; Yanagisawa, K.; Michikawa, M. Promotion of tau phosphorylation by MAP kinase Erk1/2 is accompanied by reduced cholesterol level in detergent-insoluble membrane fraction in Niemann-Pick C1-deficient cells. *J. Neurochem.*, **2003**, *84*, 1086-1096.

[69] Ukil, A.; Kar, S.; Srivastav, S.; Ghosh, K.; Das, P.K. Curative effect of 18β-glycyrrhetinic acid in experimental visceral leishmaniasis depends on phosphatase-dependent modulation of cellular MAP kinases. *PLoS One*, **2011**, *6*, e29062.

[70] Couch, R.D.; Ganem, N.J.; Zhou, M.; Popov, V.M.; Honda, T.; Veenstra, T.D.; Sporn, M.B.; Anderson, A.C. 2-cyano-3,12-dioxooleana-1,9-(11)-diene-28-oic acid disrupts microtubule polymerization: a possible mechanism contributing to apoptosis. *Mol. Pharmacol.*, **2006**, *69*, 1158-1165.

[71] Lavhale, M.S.; Kumar, S.; Mishra, S.H.; Sitasawad, S.L. A novel triterpenoid isolated from the root bark of *Ailanthus excelsa* Roxb (Tree of Heaven), AECHL-1 as a potential anti-cancer agent. *PLoS One*, **2009**, *4*, e5365.

[72] Fridman, E.; Lichtstein, D.; Rosen, H. Formation of new high density glycogen-microtubule structures is induced by cardiac steroids. *J. Biol. Chem.*, **2012**, *287*, 6518-6529.

[73] Li, M.; Wei, S.Y.; Xu, B.; Guo, W.; Liu, D.L.; Cui, J.R.; Yao, X.S. Pro-apoptotic and microtubule-disassembly effects of ardisiacrispin (A+B), triterpenoid saponins from *Ardisia crenata* on human hepatoma Bel-7402 cells. *J. Asian. Nat. Prod. Res.*, **2008**, *10*, 739-746.

[74] Saleem, M.; Murtaza, I.; Witkowsky, O.; Kohl, A.M.; Maddodi, N. Lupeol triterpene, a novel diet-based microtubule targeting agent: disrupts survivin/cFLIP activation in prostate cancer cells. *Biochem. Biophys. Res. Commun.*, **2009**, *388*, 576-582.

[75] Boykin, C.; Zhang, G.; Chen, Y.H.; Zhang, R.W.; Fan, X.E.; Yang, W.M.; Lu, Q. Cucurbitacin IIa: a novel class of anti-cancer drug inducing non-reversible actin aggregation and inhibiting survivin independent of JAK2/STAT3 phosphorylation. *Br. J. Cancer*, **2011**, *104*, 781-789.

[76] Zhang, Y.; Ouyang, D.; Xu, L.; Ji, Y.; Zha, Q.; Cai, J.; He, X. Cucurbitacin B induces rapid depletion of the G-actin pool through reactive oxygen species-dependent actin aggregation in melanoma cells. *Acta Biochim. Biophys. Sin.*, **2011**, *43*, 556-567.

[77] Ma, R.; Song, G.; You, W.; Yu, L.; Su, W.; Liao, M.; Zhang, Y.; Huang, L.; Zhang, X.; Yu, T. Anti-microtubule activity of tubeimoside I and its colchicine binding site of tubulin. *Cancer Chemother. Pharmacol.*, **2008**, *62*, 559-568.

[78] Goswami, C.; Kuhn, J.; Dina, O.A.; Fernández-Ballester, G.; Levine, J.D.; Ferrer-Montiel, A.; Hucho, T. Estrogen destabilizes microtubules through an ion-conductivity-independent TRPV1 pathway. *J. Neurochem.*, **2011**, *117*, 995-1008.

[79] Xu, Z.W.; Wang, F.M.; Gao, M.J.; Chen, X.Y.; Shan, N.N.; Cheng, S.X.; Mai, X.; Zala, G.H.; Hu, W.L.; Xu, R.C. Cardiotonic steroids attenuate ERK phosphorylation and generate cell cycle arrest to block human hepatoma cell growth. *J. Steroid Biochem. Mol. Biol.*, **2011**, *125*, 181-191.

[80] Welch, L.C.; Lecuona, E.; Briva, A.; Trejo, H.E.; Dada, L.A.; Sznajder, J.I. Extracellular signal-regulated kinase (ERK) participates in the hypercapnia-induced Na, K-ATPase downregulation. *FEBS Lett.*, **2010**, *584*, 3985-3989.

[81] Chen, Y.; Li, X.; Ye, Q.; Tian, J.; Jing, R.; Xie, Z. Regulation of alpha1 Na/K-ATPase expression by cholesterol. *J. Biol. Chem.*, **2011**, *286*, 15517-15524.

[82] Almeida-Amaral, E.E.; Caruso-Neves, C.; Lara, L.S.; Pinheiro, C.M.; Meyer-Fernandes, J.R. *Leishmania amazonensis*: PKC-like protein kinase modulates the ($Na^{++}K^{+}$)ATPase activity. *Exp. Parasitol.*, **2007**, *116*, 419-426.

[83] Yoon, S.; Seger, R. The extracellular signal-regulated kinase: multiple substrates regulate diverse cellular functions. *Growth Factors*, **2006**, *24*, 21-44.

[84] Feng, G.J.; Goodridge, H.S.; Harnett, M.M.; Wei, X.Q.; Nikolaev, A.V.; Higson, A.P.; Liew, F.Y. Extracellular signal-related kinase (ERK) and p38 mitogen-activated protein (MAP) kinases differentially regulate the lipopolysaccharide-mediated induction of inducible nitric oxide synthase and IL-12 in macrophages: *Leishmania* phosphoglycans subvert macrophage IL-12 production by targeting ERK MAP kinase. *J. Immunol.*, **1999**, *163*, 6403-6412.

[85] Martiny, A.; Meyer-Fernandes, J.R.; de Souza, W.; Vannier-Santos, M.A. Altered tyrosine phosphorylation of ERK1 MAP kinase and other macrophage molecules caused by *Leishmania* amastigotes. *Mol. Biochem. Parasitol.*, **1999**, *102*, 1-12.

[86] Privé, C.; Descoteaux, A. *Leishmania donovani* promastigotes evade the activation of mitogen-activated protein kinases p38, c-Jun N-terminal kinase, and extracellular signal-regulated kinase-1/2 during infection of naive macrophages. *Eur. J. Immunol.*, **2000**, *30*, 2235-2244.

[87] Parsons, M.; Worthey, E.A.; Ward, P.N.; Mottram, J.C. Comparative analysis of the kinomes of three pathogenic trypanosomatids: *Leishmania major*, *Trypanosoma brucei* and *Trypanosoma cruzi*. *BMC Genomics*, **2005**, *6*, 127.

[88] Saravanan, P.; Venkatesan, S.K.; Mohan, C.G.; Patra, S.; Dubey, V.K. Mitogen-activated protein kinase 4 of *Leishmania* parasite as a therapeutic target. *Eur. J. Med. Chem.*, **2010**, *45*, 5662-5670.

[89] Brumlik, M.J.; Pandeswara, S.; Ludwig, S.M.; Murthy, K.; Curiel, T.J. Parasite mitogen-activated protein kinases as drug discovery targets to treat human protozoan pathogens. *J. Signal Transduct.*, **2011**, 968-971.

[90] Kumari, S.; Singh, S.; Saha, B.; Paliwal, P.K. *Leishmania major* MAP kinase 10 is protective against experimental *L. major* infection. *Vaccine*, **2011**, *29*, 8783-8787.

[91] Rotureau, B.; Morales, M.A.; Bastin, P.; Späth, G.F. The flagellum-mitogen-activated protein kinase connection in trypanosomatids: a key sensory role in parasite signalling and development? *Cell Microbiol.*, **2009**, *11*, 710-718.

[92] Van Den Abbeele, J.; Claes, Y.; van Bockstaele, D.; Le Ray, D.; Coosemans, M. *Trypanosoma brucei* spp. development in the tsetse fly: characterization of the post-mesocyclic stages in the foregut and proboscis. *Parasitology*, **1999**, *118*, 469-478.

[93] de Souza, W. Basic cell biology of *Trypanosoma cruzi*. *Curr. Pharm. Des.*, **2002**, *8*, 269-285.

[94] Martiny, A.; Vannier-Santos, M.A.; Borges, V.M.; Meyer-Fernandes, J.R.; Assreuy, J.; Cunha e Silva, N.L.; de Souza, W. *Leishmania*-induced tyrosine phosphorylation in the host macrophage and its implication to infection. *Eur. J. Cell Biol.*, **1996**, *71*, 206-215.

[95] Quarmby, L.M.; Parker, J.D. Cilia and the cell cycle? *J. Cell Biol.*, **2005**, *169*, 707-710.

[96] Parker, J.D.; Bradley, B.A.; Mooers, A.O.; Quarmby, L,M. Phylogenetic analysis of the Neks reveals early diversification of ciliary-cell cycle kinases. *PLoS One*, **2007**, *2*, e1076.

[97] Ralston, K.S.; Hill, K.L. The Flagellum of *Trypanosoma brucei*: New tricks from an old dog. *Int. J. Parasitol.*, **2008**, *38*, 869-884.

[98] Robinson, D.R.; Gull, K. Basal body movements as a mechanism for mitochondrial genome segregation in the trypanosome cell cycle. *Nature*, **1991**, *352*, 731-733.

[99] Robinson, D.R.; Sherwin, T.; Ploubidou, A.; Byard, E.H.; Gull, K. Microtubule polarity and dynamics in the control of organelle positioning, segregation, and cytokinesis in the trypanosome cell cycle. *J. Cell Biol.*, **1995**, *128*, 1163-1172.

[100] Christensen, S.T.; Clement, C.A.; Satir, P.; Pedersen, L.B. Primary cilia and coordination of receptor tyrosine kinase (RTK) signalling. *J. Pathol.*, **2012**, *226*, 172-184.

[101] Vannier-Santos, M.A.; Martiny, A.; de Souza, W. Cell biology of *Leishmania* spp.: invading and evading. *Curr. Pharm. Des.*, **2002**, *8*, 297-318.

[102] Field, M.C.; Carrington, M. The trypanosome flagellar pocket. *Nat. Rev. Microbiol.*, **2009**, *7*, 775-786.

[103] Molla-Herman, A.; Ghossoub, R.; Blisnick, T.; Meunier, A.; Serres, C.; Silbermann, F.; Emmerson, C.; Romeo, K.; Bourdoncle, P.; Schmitt, A.; Saunier, S.; Spassky, N.; Bastin, P.; Benmerah, A. The ciliary pocket: an endocytic membrane domain at the base of primary and motile cilia. *J. Cell Sci.*, **2010**, *15*, 1785-1795.

[104] Hoey, D.A.; Downs, M.E.; Jacobs, C.R. The mechanics of the primary cilium: an intricate structure with complex function. *J. Biomech.*, **2012**, *45*, 17-26.

[105] Pampliega, O.; Orhon, I.; Patel, B.; Sridhar, S.; Díaz-Carretero, A.; Beau, I.; Codogno, P.; Satir, B.H.; Satir, P.; Cuervo, A.M. Functional interaction between autophagy and ciliogenesis. *Nature*, **2013**, *502*,194-200.

[106] Lohret, T.A.; Zhao, L.; Quarmby, L.M. Cloning of *Chlamydomonas* p60 katanin and localization to the site of outer doublet severing during deflagellation. *Cell Motil. Cytoskeleton*, **1999**, *43*, 221-231.

[107] Quarmby, L. Cellular samurai: katanin and the severing of microtubules. *J. Cell Sci.*, **2000**, *113*, 2821–2827.

[108] Mahjoub, M.R.; Montpetit, B.; Zhao, L.; Finst, R.J.; Goh, B.; Kim, A.C.; Quarmby, L.M. The FA2 gene of *Chlamydomonas* encodes a NIMA family kinase with roles in cell cycle progression and microtubule severing during deflagellation. *J. Cell Sci.*, **2002**, *15*, 1759-1768.

[109] Quarmby, L.M. Cellular deflagellation. *Int. Rev. Cytol.*, **2004**, *233*, 47–91.

[110] Selvapandiyan, A.; Kumar, P.; Morris, J.C.; Salisbury, J.L.; Wang, C.C.; Nakhasi, H.L. Centrin1 is required for organelle segregation and cytokinesis in *Trypanosoma brucei*. *Mol. Biol. Cell*, **2007**, *18*, 3290-3301.

[111] Meraldi, P.; Nigg, E.A. Centrosome cohesion is regulated by a balance of kinase and phosphatase activities. *J. Cell Sci.*, **2001**, *114*, 3749-3757.

[112] Mazzorana, M.; Montoya, G.; Mortuza, G.B. The centrosome: a target for cancer therapy. *Curr. Cancer Drug Targets*, **2011**, *11*, 600-612.

[113] Anderhub, S.J.; Krämer, A.; Maier, B. Centrosome amplification in tumorigenesis. *Cancer Lett.*, **2012**, *322*, 8-17.

[114] Ogbadoyi, E.O.; Robinson, D.R.; Gull, K. A high-order transmembrane structural linkage is responsible for mitochondrial genome positioning and segregation by flagellar basal bodies in trypanosomes. *Mol. Biol. Cell*, **2003**, *14*, 1769-1779.

[115] Vannier-Santos, M.A.; Urbina, J.A.; Martiny, A.; Neves, A.; de Souza, W. Alterations induced by the antifungal compounds ketoconazole and terbinafine in *Leishmania*. *J. Eukaryot. Microbiol.*, **1995**, *42*, 337-346.

[116] Vannier-Santos, M.A.; Martiny, A.; Lins, U.; Urbina, J.A.; Borges, V.M.; de Souza, W. Impairment of sterol biosynthesis leads to phosphorus and calcium accumulation in *Leishmania* acidocalcisomes. *Microbiology*, **1999**, *145*, 3213-3220.

[117] Newman, R.A.; Kondo, Y.; Yokoyama, T.; Dixon, S.; Cartwright, C.; Chan, D.; Johansen, M.; Yang, P. Autophagic cell death of human pancreatic tumor cells mediated by oleandrin, a lipid-soluble cardiac glycoside. *Integr. Cancer Ther.*, **2007**, *6*, 354-364.

[118] Xu, Z.X; Liang, J.; Haridas, V.; Gaikwad, A.; Connolly, F.P.; Mills, G.B.; Gutterman, J.U. A plant triterpenoid, avicin D, induces autophagy by activation of AMP-activated protein kinase. *Cell Death Differ.*, **2007**, *14*, 1948-1957.

[119] Wang, H.; Haridas, V.; Gutterman, J.U.; Xu, Z.X. Natural triterpenoid avicins selectively induce tumor cell death. *Commun. Integr. Biol.*, **2010**, *3*, 205-208.

[120] Shin, S.W.; Kim, S.Y.; Park, J.W. Autophagy inhibition enhances ursolic acid-induced apoptosis in PC3 cells. *Biochim. Biophys. Acta*, **2012**, *1823*, 451-457.

[121] Xie, C.M.; Chan, W.Y.; Yu, S.; Zhao, J.; Cheng, C.H. Bufalin induces autophagy-mediated cell death in human colon cancer cells through reactive oxygen species generation and JNK activation. *Free Radic. Biol. Med.*, **2011**, *51*, 1365-1375.

[122] Tabas, I. A two-carbon switch to sterol-induced autophagic death. *Autophagy*, **2007**, *3*, 38-41.

[123] Lima, J.G.; de Freitas Vinhas, C.; Gomes, I.N.; Azevedo, C.M.; dos Santos, R.R.; Vannier-Santos, M.A.; Veras, P.S. Phagocytosis is inhibited by autophagic induction in murine macrophages. *Biochem. Biophys. Res. Commun.*, **2011**, *405*, 604-609.

[124] Cunha, S.D.; Bastos, R.M.; Silva, P.O.; Costa, G.A.N.; Vencato, I.; Lariucci, C.; Napolitano, H.B.; Oliveira, C.M.A.; Kato, L.; Silva, C.C.; Menezes, D.; Vannier-Santos, M.A. Synthesis and Structural Studies of 4-Thioxopyrimidines with Antimicrobial Activities. *Monatsh. Chem.*, **2007**, *138*, 111-119.

[125] Bernardino, A.M.; da Silva Pinheiro, L.C.; Rodrigues, C.R.; Loureiro, N.I.; Castro, H.C.; Lanfredi-Rangel, A.; Sabatini-Lopes, J.; Borges, J.C.; Carvalho, J.M.; Romeiro, G.A.; Ferreira, V.F.; Frugulhetti, I.C.; Vannier-Santos, M.A. Design, synthesis, SAR, and biological evaluation of new 4-(phenylamino)thieno[2,3-b]pyridine derivatives. *Bioorg. Med. Chem.*, **2006,** *14*, 5765-5770

Received: May 18, 2013 **Revised: March 05, 2014** **Accepted: March 06, 2014**